Photoluminescence of Homoleptic Lanthanide Complexes With Tris(benzotriazol-1-yl)borate

Marco Bortoluzzi[1] · **Valentina Ferraro[1]** · **Federica Sartor[1]**

Abstract

Bright photoluminescent neutral complexes having general formula $[Ln(tbtz)_3]$ (Ln = Eu, Tb; tbtz = tris(benzotriazol-1-yl) borate) were obtained by reacting K[tbtz] with $EuCl_3$ and $TbCl_3$. The emissions in the visible range, related to the f-f transitions of the trivalent lanthanide ions, are observable upon excitation with wavelengths shorter than 350 nm. The most intense emission bands correspond to the $^5D_0 \rightarrow {}^7F_4$ transition at 699 nm for the europium complex and to the $^5D_4 \rightarrow {}^7F_5$ transition at 542 nm for the terbium derivative. The luminescence is in all the cases mostly associated with the antenna-effect from the coordinated tbtz ligands. The synthetic approach was successfully extended to the preparation of the analogous yttrium and gadolinium derivatives. Tricapped trigonal prismatic geometry was attributed to the complexes on the basis of luminescence data and DFT calculations. Highly photoluminescent plastic materials were obtained by embedding small amounts of $[Eu(tbtz)_3]$ or $[Tb(tbtz)_3]$ in poly(methyl methacrylate).

Keyword Lanthanides · Scorpionates · Ln^{3+} transitions · Benzotriazole · Doped polymers

Introduction

Luminescent complexes of trivalent lanthanide ions are of widespread interest for advanced technologies [1–5]. Selected examples of application include electronic devices [6, 7], electroluminescent materials [8, 9], photovoltaics [10], biological probes and multifunctional materials [11–20].

Poly(pyrazol-1-yl)borate ligands were widely employed for the preparation of lanthanide complexes, that were investigated for their structural, magnetic and luminescent features [21–32]. In particular, coordination compounds having the general formula $[Ln(Tp)_3]$, where Tp is tris(pyrazol-1-yl)borate, were characterized by means of single crystal X-ray diffraction. It was observed that the metal centre in homoleptic tris(pyrazol-1-yl)borate lanthanide complexes can be nine- or eight-coordinated depending upon its ionic radius. The electronic structures of the lanthanide centres were investigated in detail and antenna-effect was detected

for some visible- and NIR-emitting complexes [33–39]. The pure complexes showed high thermal stability [39]. Appreciable photoluminescence was maintained also after dispersion in acrylic-based polymers, or after mixing the complexes with different inorganic pigments and suitable binders [40, 41].

The functionalization of the poly(pyrazol-1-yl)borate skeleton demonstrated to be a viable route for the preparation of new luminescent lanthanide complexes. For instance, the coordination of bis[3-(2-pyridyl)pyrazol-1-yl]dihydroborate to Yb(III), Nd(III) and Er(III) afforded NIR-emitting species. The analogous Pr(III) derivative showed luminescence both in the NIR and in the visible regions [42].

Another approach to prepare new scorpionate-based luminescent compounds is the replacement of the pyrazol-1-yl moieties with azoles characterized by different donor ability and steric bulk, together with improved light-harvesting properties [43]. In this paper we describe the straightforward preparation of new homoleptic lanthanide complexes with tris(benzotriazol-1-yl)borate in the coordination sphere. Particular attention was devoted to the photophysical characterization of the europium and terbium complexes, that allowed to highlight analogies and differences with the homoleptic tris(pyrazol-1-yl)borate complexes already reported. Finally, the new compounds were studied as dopants for the preparation of photoluminescent polymers.

✉ Marco Bortoluzzi
markos@unive.it

1 Dipartimento di Scienze Molecolari e Nanosistemi, Università Ca' Foscari Venezia, Via Torino 155, 30172 Mestre, VE, Italy

Experimental Section

Chemicals

Commercial organic solvents (toluene ≥ 99.5%, diethyl ether ≥ 99.7%, dichloromethane ≥ 99.8%) were purchased from Sigma Aldrich (Germany) and purified with Na/benzophenone (toluene, diethyl ether) or CaH_2 (dichloromethane) following literature methods [44]. 1*H*-benzotriazole (≥ 99.0%) and potassium borohydride (98%) were Sigma Aldrich (Germany) products, used as received. Yttrium and lanthanide chlorides (99.9% in all the cases) were Strem Chemicals (France) products, used without further purifications. Poly(methyl methacrylate) (PMMA, $M_w = 86,000$ g mol^{-1}) was purchased from TCI Chemicals (Belgium) and used as received. Potassium tris(benzotryazol-1-yl)borate, K[tbtz], was synthesized accordingly to literature procedures [45–47].

Characterization Methods

Elemental analyses (C, H, N) were carried out using an Elementar micro elemental analyzer, model UNICUBE® (Germany). Magnetic susceptibilities were measured on solid samples at 298 K with a Sherwood Scientific magnetic susceptibility balance, model MK1 (UK), and corrected for diamagnetic contribution by means of tabulated Pascal's constants [48]. Conductivity measurements were carried out using a Radiometer Copenhagen instrument, model CDM83 (Denmark). IR spectra were collected in the $4000 - 400$ cm^{-1} range using a Perkin-Elmer spectrophotometer, model Spectrum One (UK). ^{1}H NMR spectra were recorded with a Bruker instrument operating at 300.13 MHz, model Avance 300 (Germany). The spectra were recorded in deuterated dimethylsulfoxide (99.90% D, Eurisotop, France), used as received. The ^{1}H NMR chemical shifts were referred to the partially deuterated fraction of the solvent (2.50 ppm), itself quoted with respect to tetramethylsilane ($\delta = 0.00$ ppm).

Absorption spectra in dichloromethane solution were collected using a Perkin-Elmer spectrophotometer, model Lambda 35 (UK). Photoluminescence emission (PL) and excitation (PLE) measurements were carried out at room temperature on solid samples by a Horiba Jobin Yvon spectrofluorometer, model Fluorolog-3 (France). A continuous-wave xenon arc lamp was used as source selecting the excitation wavelength by a double Czerny-Turner monochromator. A single grating monochromator coupled to a Hamamatsu Photonics R928 photomultiplier tube (Japan) was used as detection system for optical emission measurements. Excitation and emission spectra were corrected for the instrumental functions. Time-resolved analyses were performed in Multi

Channel Scaling modality (MCS, 3000 channels, 5000 ns/channel) by using a pulsed Ekspla NT/342 Nd:YAG laser (Lithuania) equipped with an optical parametric oscillator. The pulse duration of the laser was 6 ns and the repetition rate was 10 Hz. The channels related to the time before and during the excitation pulse were removed from the subsequent analysis.

Synthesis of [Ln(tbtz)₃] Complexes (Ln = Y, Eu, Gd, Tb) and Doped Polymers

YCl_3 or $LnCl_3$ (Ln = Eu, Gd, Tb) (5.0 mmol) was dissolved in 10 mL of distilled water. 5 mL of 0.1 M HCl was then added. A solution containing 1.5 mmol (0.608 g) of K[tbtz] in 20 mL of H_2O was slowly added to the reaction mixture. After 24 h under stirring at room temperature the white solid formed was collected by filtration, washed with 5 mL of water and dried under vacuum in the presence of P_4O_{10}. The product was purified by dissolution in hot toluene (100 mL), and the solution thus obtained was quickly filtered to remove the residual particulate. The solvent was then removed under reduced pressure. The addition of diethyl ether (20 mL) caused the separation of a white solid, that was collected by filtration, washed with 5 mL of diethyl ether and dried under vacuum. Yield ≥ 70% in all the cases.

Doped polymers, generally indicated as [Ln(tbtz)₃]@PMMA, were prepared from dichloromethane solutions of the complexes and commercial PMMA. In a typical preparation, a weighed amount of [Ln(tbtz)₃] (from 0.020 to 0.060 g) was dissolved in 5 mL of dichloromethane. The solution was added to a gently stirred solution of PMMA (1.000 g) in 40 mL of CH_2Cl_2. The solution was then concentrated at a reduced pressure to about 3 mL and transferred into a round polyethylene holder having 1 cm diameter. The residual solvent was allowed to evaporate in air at room temperature. The final plastic material was kept under vacuum overnight to remove the traces of solvent.

Characterization of [Ln(tbtz)₃] Complexes

Ln = Y. Anal. calcd for $C_{54}H_{39}B_3N_{27}Y$ (1187.41 g mol^{-1}, %): C, 54.62; H, 3.31; N, 31.85. Found (%): C, 54.39; H, 3.33; N, 31.72. IR (cm^{-1}): 2426 (ν_{BH}). ^{1}H NMR (DMSO-d_6, 298 K) δ: 7.78 (2 dd, 2H, $^3J_{HH} = 7.1$ Hz, $^4J_{HH} = 1.3$ Hz, benzotriazole-H5 and benzotriazole-H6); 7.26, 7.13 (2 td, 2H, $^3J_{HH} = 7.1$ Hz, $^4J_{HH} = 1.3$ Hz, benzotriazole-H4 and benzotriazole-H7).

Ln = Eu. Anal. calcd for $C_{54}H_{39}B_3N_{27}Eu$ (1250.47 g mol^{-1}, %): C, 51.87; H, 3.14; N, 30.24. Found (%): C, 51.66; H, 3.18; N, 30.10. χ^M_{corr} (c.g.s.u., 298 K): $4.85 \cdot 10^{-3}$. IR (cm^{-1}): 2431 (ν_{BH}). ^{1}H NMR (DMSO-d_6, 298 K) δ: 7.80 (2 d, slightly br, 2H, $^3J_{HH} = 6.8$ Hz, benzotriazole-H5 and benzotriazole-H6); 7.28, 7.15 (2

t, slightly br, 2H, $^3J_{HH} = 6.8$ Hz, benzotriazole-H4 and benzotriazole-H7).

Ln = Gd. Anal. calcd for $C_{54}H_{39}B_3N_{27}Gd$ (1255.75 g mol^{-1}, %): C, 51.65; H, 3.13; N, 30.12. Found (%): C, 51.44; H, 3.17; N, 29.98. χ^M_{corr} (c.g.s.u., 298 K): $2.64 \cdot 10^{-2}$. IR (cm^{-1}): 2431 (ν_{BH}).

Ln = Tb. Anal. calcd for $C_{54}H_{39}B_3N_{27}Tb$ (1257.43 g mol^{-1}, %): C, 51.58; H, 3.13; N, 30.08. Found (%): C, 51.37; H, 3.18; N, 29.96. χ^M_{corr} (c.g.s.u., 298 K): $4.03 \cdot 10^{-2}$. IR (cm^{-1}): 2431 (ν_{BH}). ^{1}H NMR (DMSO-d$_6$, 298 K) δ: 7.82, 7.67, 7.21, 7.08 (4 s, br, 4H, benzotriazole hydrogen atoms).

Computational Details

The computational geometry optimizations were carried out without symmetry constraints using the hybrid-GGA DFT functional EDF2 [49], in combination with the split-valence polarized 6–31G(d,p) basis set for light atoms and the LANL2DZ basis set for yttrium [50]. The scalar quasirelativistic 4f-in-core pseudopotentials ECP52MWB, ECP53MWB and ECP54MWB were used respectively for europium, gadolinium and terbium, with the associated valence basis sets [51–53]. Because of the inclusion of the 4f^n shell of Ln(III) in the pseudopotential, the "restricted" formalism was applied [54]. Calculations were performed with Spartan'16 (Wavefunction Inc., USA), build 2.0.3 [55], running on Intel Xeon-based x86–64 workstations.

Results and Discussion

Homoleptic tris(benzotriazol-1-yl) borate lanthanide complexes having general formula [Ln(tbtz)$_3$] (Ln = Y, Eu, Tb) were easily synthesized from the reaction of the corresponding metal chlorides and three equivalents of K[tbtz] in slightly acidic water (Scheme 1). They were purified by dissolution in hot toluene, followed by precipitation with diethyl ether. Elemental analysis data are in agreement with the proposed formulations and dichloromethane solutions of the complexes are non-conductive. The experimental magnetic moments at room temperature are 3.3 BM for [Eu(tbtz)$_3$] and 9.8 BM for [Tb(tbtz)$_3$], in agreement with the values expected for complexes of trivalent europium and terbium ions [56]. The IR spectra are closely comparable and show a band around 2430 cm^{-1} attributable to ν_{B-H} stretching. The ^{1}H NMR spectra in DMSO-d$_6$ at room temperature are composed by two superimposed doublets and two triplets for the benzotrazol-1-yl groups, indicating that all the coordinating moieties are equivalent on the NMR timescale. The presence of paramagnetic centres causes the expected broadening of the resonances.

The UV–VIS spectra of the complexes show intense absorptions for wavelengths below 300 nm (Fig. 1), with maxima around 278 nm and molar extinction coefficients close to 40,000 M^{-1} cm^{-1}. [Eu(tbtz)$_3$] and [Tb(tbtz)$_3$] are appreciably photoluminescent under UV irradiation, both as solid samples and in dichloromethane solution. The PL spectrum of [Eu(tbtz)$_3$] reported in Fig. 1 is composed by

Scheme 1 Synthesis of [Ln(tbtz)$_3$] complexes

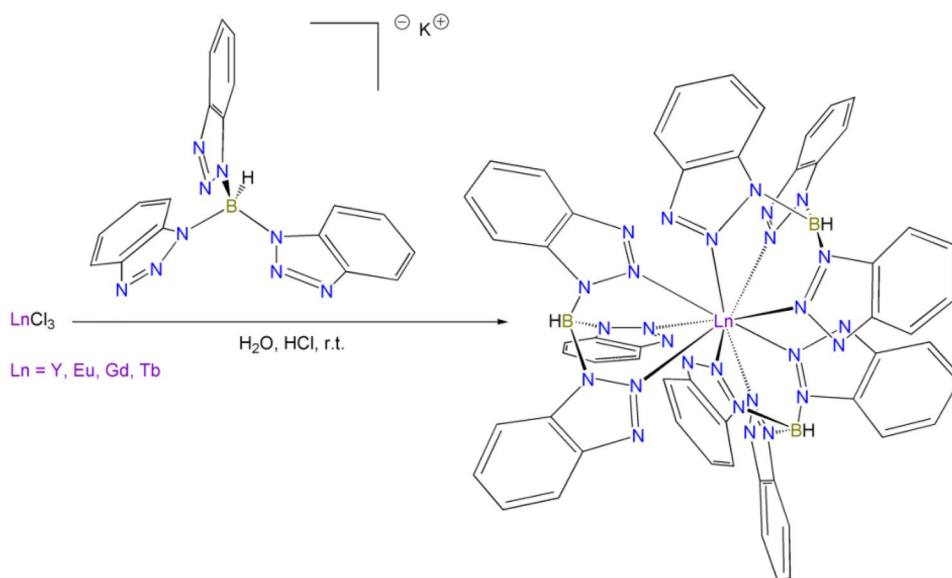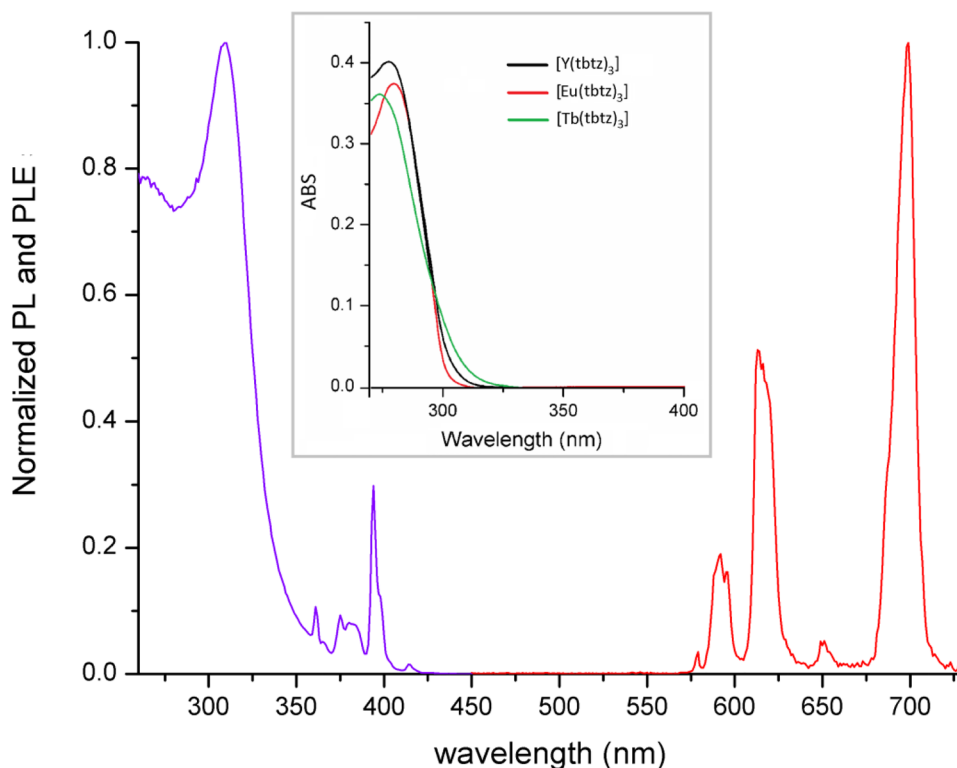**Fig. 1** PL (red line, $\lambda_{excitation} = 310$ nm) and PLE (violet line, $\lambda_{emission} = 700$ nm) of solid [Eu(tbtz)$_3$] at room temperature. Inset: absorption spectra of 10^{-5} M CH$_2$Cl$_2$ solutions of [Ln(tbtz)$_3$] complexes


the typical $^5D_0 \to {}^7F_J$ (J = 0 – 4) transitions of the metal centre between 580 and 700 nm, without any signal attributable to luminescence from the coordinated ligands. The related PLE spectrum (Fig. 1) shows a noticeable antenna-effect for wavelengths below 350 nm, with a maximum at 309 nm. The dominant contribution of coordinated tbtz to the sensitization of Eu(III) luminescence is evidenced by the relative intensity of the ligand-related band with respect to the direct excitations of the metal centre, the $^5L_6 \leftarrow {}^7F_0$ at 394 nm in particular. The presence of a single $^5D_0 \to {}^7F_0$ band at 579 nm in the PL spectrum suggests the presence of only one emitting species, even if such information is not conclusive [57]. The relatively low intensity of the $^5D_0 \to {}^7F_2$ hypersensitive band centred around 616 nm and the quite low I($^5D_0 \to {}^7F_2$):I($^5D_0 \to {}^7F_1$) intensity ratio, around 3:1, indicate a symmetric coordination sphere surrounding the metal ion. The most intense band, corresponding to about 60% of the total emission, is the $^5D_0 \to {}^7F_4$ one, centred at 699 nm. Such a feature is relatively uncommon and it was observed for instance for the tris(pyrazol-1-yl)borate complex [Eu(Tp)$_3$] [39]. The relative intensities of the transitions in the PL spectrum suggest that [Eu(tbtz)$_3$] is nine-coordinated. The separation in three m$_J$ sublevels of the I($^5D_0 \to {}^7F_1$) band does not rule out this hypothesis, because the separation is predicted also for the D_{2h} symmetry point group characteristic of a regular tricapped trigonal prism [57].

Despite the fact that we were unable to obtain crystals suitable for X-Ray diffraction, the DFT-optimized geometry of [Eu(tbtz)$_3$] confirms the proposed geometry for the complex, and the tricapped trigonal prism is predicted also for the first coordination sphere of analogous yttrium derivative, [Y(tbtz)$_3$]. The computed ground-state geometry of [Eu(tbtz)$_3$] is shown in Fig. 2. Selected computed bond lengths are collected in the caption of Fig. 2.

The emission of [Eu(tbtz)$_3$] falls in the reddish orange region of the CIE 1931 diagram with unitary colour purity, as shown in Fig. 3 [58]. The luminescence decay curve is monoexponential, as observable from the semi-log plot reported in Fig. 3. The measured lifetime value (τ) is 0.341 ms. The intrinsic quantum yield Q_{Eu}^{Eu} was estimated from the lifetime value on the basis of equation (1), where n indicates the refractive index of the sample. The value of 1.5 is assumed for solid state samples in this work fo comparative purposes [59], even if it is worth noting that refractive index may differ depending on the nature of the sample. I($^5D_0 \to {}^7F_J$)/I($^5D_0 \to {}^7F_1$) is the ratio between the total integrated emission from the Eu($^5D_0$) level to the ^7F_J manifold and the integrated intensity of the transition $^5D_0 \to {}^7F_1$ [59].

$$Q_{Eu}^{Eu} = 14.65 \, n^3 \frac{I(^5D_0 \to {}^7F_J)}{I(^5D_0 \to {}^7F_1)} \tau(s) \qquad (1)$$

Fig. 2 DFT-optimized geometry of [Eu(tbtz)$_3$]. Hydrogen atoms are omitted for clarity. Inset: tricapped trigonal prism surrounding the Eu(III) centre. Colour map: Eu, violet; N, blue; C, grey; B, yellow. Selected computed Ln-N bond lengths (Á): [Eu(tbtz)$_3$], 2.511 – 2.515 (trigonal prism), 2.729 – 2.742 (capped); [Gd(tbtz)$_3$], 2.497 – 2.502 (trigonal prism), 2.735 – 2.739 (capped); [Tb(tbtz)$_3$], 2.484 – 2.488 (trigonal prism), 2.720 – 2.736 (capped); [Y(tbtz)$_3$], 2.493 – 2.497 (trigonal prism), 2.725 – 2.741 (capped)
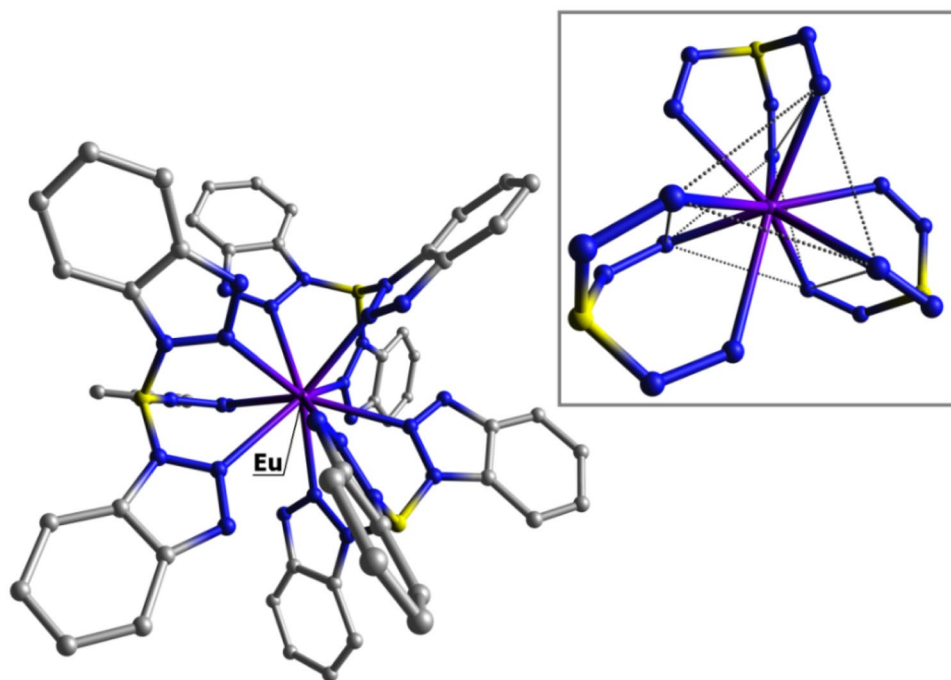
The Q_{Eu}^{Eu} value for solid [Eu(tbtz)$_3$] is 19%. The τ value is much lower than the reference value of 1.84 ms obtained for [Eu(Tp)$_3$] under comparable conditions. As a consequence, also the intrinsic quantum yield is lower, being that of [Eu(Tp)$_3$] around 43% [39]. Despite this limitation, the formal replacement of pyrazol-1-yl substituents with benzotriazol-1-yl broadens the absorption spectrum towards longer wavelengths and increases the absorption coefficients with respect to [Eu(Tp)$_3$], making the complex bright photoluminescent. Luminescence data are collected in Table 1.

Another difference of [Eu(tbtz)$_3$] with respect to [Eu(Tp)$_3$] is that water suspensions of the last compound

Fig.3 Semi-log plot of the luminescence decay curve of [Eu(tbtz)$_3$] (red line) and monoexponential fit (black line). Solid sample, r.t., $\lambda_{excitation} = 310$ nm, $\lambda_{emission} = 700$ nm. Inset: CIE 1931 chromaticity diagram
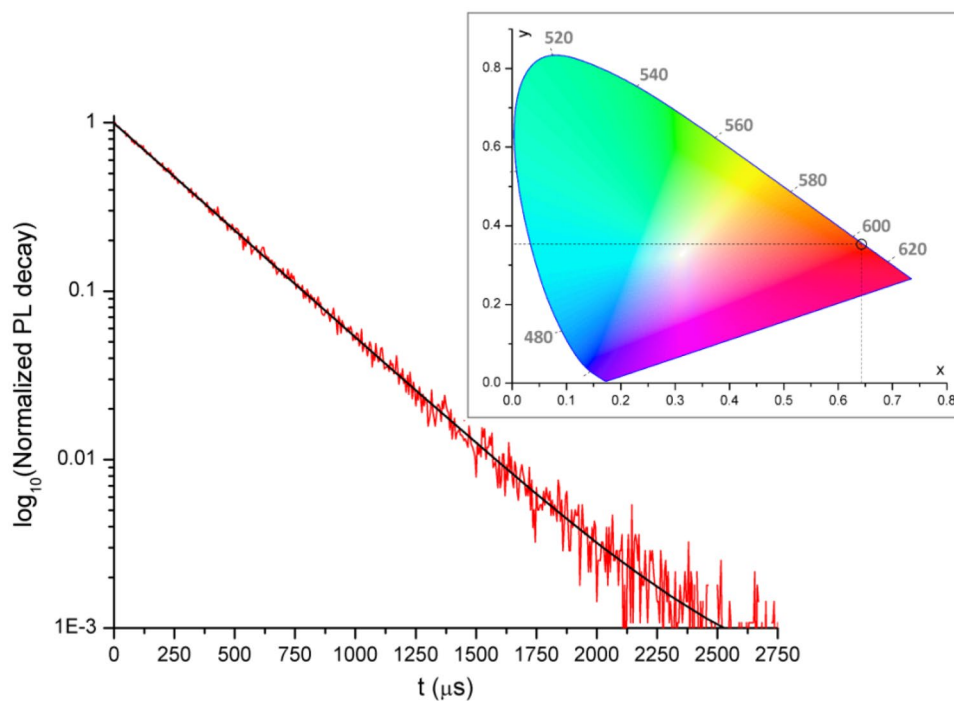
Table 1 Absorption and emission data of the complexes and of the doped polymers

Compound	[a] UV–VIS, nm (ε, cm^{-1} M^{-1})	[b] PL, nm	[b] PLE, nm	[b] τ(ms)	Q_{Ln}^{Ln}(%)	CIE
[Y(tbtz)$_3$]	278 (40,100)	——	——	——	——	——
[Eu(tbtz)$_3$]	280 (37,400)	[c] 579 ($^5D_0 \to {}^7F_0$, 0.8%) 588, 592, 596 ($^5D_0 \to {}^7F_1$, 8.8%) 613, 616 ($^5D_0 \to {}^7F_2$, 28.1%) 649, 651 ($^5D_0 \to {}^7F_3$, 2.4%) 699 ($^5D_0 \to {}^7F_4$, 59.9%)	[d] $\leq$350 (ligand excitation, max 309) 361, 375, 383 (Eu^{3+} excitation) 394 ($^5L_6 \leftarrow {}^7F_0$ Eu^{3+} excitation)	[c,d] 0.341	19	x = 0.643 y = 0.353
[Gd(tbtz)$_3$]	276 (36,800)	[e] 364 very weak	——	[f,g] $<5 \cdot 10^{-4}$	——	——
[Tb(tbtz)$_3$]	274 (36,100)	[c] 489 ($^5D_0 \to {}^7F_6$, 16.9%) 542 ($^5D_0 \to {}^7F_5$, 58.8%) 583, 587 ($^5D_0 \to {}^7F_4$, 14.1%) 620 ($^5D_0 \to {}^7F_3$, 10.2%)	[h] $\leq$343 (ligand excitation, max 307) 350, 367, 378 (Tb^{3+} excitation)	[f,i] 0.383	9	x = 0.354 y = 0.566
[Eu(tbtz)$_3$]@PMMA	——	[c] 579 ($^5D_0 \to {}^7F_0$, 0.9%) 588, 594 ($^5D_0 \to {}^7F_1$, 11.7%) 612, 617 ($^5D_0 \to {}^7F_2$, 37.2%) 650 ($^5D_0 \to {}^7F_3$, 2.7%) 695, 700 ($^5D_0 \to {}^7F_4$, 47.5%)	[d] $\leq$350 (ligand excitation, max 309) 361 (Eu^{3+} excitation) 394 ($^5L_6 \leftarrow {}^7F_0$ Eu^{3+} excitation)	[c,d] 0.370	16	x = 0.646 y = 0.351
[Tb(tbtz)$_3$]@PMMA	——	[c] 489 ($^5D_0 \to {}^7F_6$, 18.2%) 544 ($^5D_0 \to {}^7F_5$, 56.7%) 583 ($^5D_0 \to {}^7F_4$, 15.2%) 621 ($^5D_0 \to {}^7F_3$, 9.9%)	[h] $\leq$350 (ligand excitation, max 311) 351, 368, 378 (Tb^{3+} excitation)	[f,i] 0.630	13	x = 0.355 y = 0.571

[a] CH$_2$Cl$_2$ solution, 298 K

[b] Solid sample, r.t

[c] $\lambda_{excitation} = 310$ nm

[d] $\lambda_{emission} = 700$ nm

[e] $\lambda_{excitation} = 280$ nm

[f] $\lambda_{excitation} = 320$ nm

[g] $\lambda_{emission} = 410$ nm

[h] $\lambda_{emission} = 542$ nm

[i] $\lambda_{emission} = 544$ nm

maintain good luminescence [41]. On the contrary, the luminescence of [Eu(tbtz)$_3$] is easily quenched by traces of water and the compound is moisture-sensitive. Such a property can be tentatively ascribed to the presence of non-coordinating nitrogen atoms in the molecular structure (N3 in the benzotriazol-1-yl skeleton), that can interact with water through hydrogen bonds, thus favouring the vibrational relaxation of the excited state. The presence of free nitrogen atoms could also explain the immediate interaction of [Eu(tbtz)$_3$] with acids in dichloromethane

solution, causing the complete quench of the luminescence (see Fig. 4).

The terbium derivative [Tb(tbtz)$_3$] shows appreciable green luminescence in dichloromethane solution and as solid sample upon excitation with UV light. DFT calculations predict a tricapped trigonal prismatic geometry strictly comparable to that obtained for the analogous europium complex. Computed data are summarized in the caption of Fig. 2. As for [Eu(tbtz)$_3$], the luminescence is quenched by water and by addition of acids to dichloromethane solutions (see Fig. 4). The PL spectrum reported in Fig. 4 shows four bands attributable to the $^5D_0 \rightarrow {}^7F_J$ (J = 6 − 3) transitions in the 450 – 650 nm range, together with weak signals at longer wavelengths related to lower J values. The most intense band falls at 542 nm and corresponds to the $^5D_0 \rightarrow {}^7F_5$ transition. The PLE spectrum (Fig. 4) is comparable to that of [Eu(tbtz)$_3$], with a strong contribution from the coordinated ligands for wavelengths below 350 nm and weak signals related to the direct excitation of Tb(III). The τ value obtained from the monoexponential fit of the luminescence decay curve is 0.383 ms. On admitting a Tb(III) radiative lifetime (τ_{rad}) of 4.75 ms [60], the intrinsic quantum yield Q_{Tb}^{Tb} is estimated on the basis of Eq. (2) around 9%. Photoluminescence data of [Tb(tbtz)$_3$] are summarized in Table 1.

$$Q_{Tb}^{Tb} = \frac{\tau(ms)}{4.75} \qquad (2)$$

The synthesis of homoleptic tbtz complexes was extended to Gd(III), in order to obtain information about the excited states of the coordinated ligands from the PL spectrum of [Gd(tbtz)$_3$]. Unfortunately, the phosphorescence of the compound is too low to be detected at room temperature, differently to what observed in the past for [Gd(Tp)$_3$] [39]. Only a very weak band centred at 364 nm is observable, attributable to fluorescence from coordinated ligands on the basis of the fast luminescence decay [61].

The appreciable photoluminescence of [Eu(tbtz)$_3$] and [Tb(tbtz)$_3$] prompted to study their use as dopants in plastic matrices, PMMA in particular. Highly photoluminescent materials were obtained with very low quantities of embedded complex, from 0.020 to 0.060 g$_{complex}$/g$_{polymer}$. The use of higher quantities of complex afforded materials with reduced transparency. Selected samples under UV light are shown in Fig. 5. The PL and PLE spectra, together with the time-resolved spectra, do not vary on changing the concentration of dopant. As observable in Fig. 5, the relative intensities of the $^5D_0 \rightarrow {}^7F_J$ transitions in the PL spectrum of [Eu(tbtz)$_3$]@PMMA are different with respect to the pure complex, suggesting that the PMMA chains alter the coordination sphere surrounding the Eu(III) centre. The most striking change is the increased intensity of the $^5D_0 \rightarrow {}^7F_2$ transition, with a peak at 612 nm. It is however worth noting that the excitations related to the tbtz ligands in the PLE spectrum are unaffected by the PMMA matrix. This last consideration is

Fig. 4 PL (green line, $\lambda_{excitation}$ = 310 nm) and PLE (violet line, $\lambda_{emission}$ = 542 nm) of solid [Tb(tbtz)$_3$] at room temperature. Picture: emissions of 10^{-4} M CH$_2$Cl$_2$ solutions of [Ln(tbtz)$_3$] (Ln = Eu, Tb) under UV light **a** and after addition of one **b** and two **c** equivalents of CH$_3$SO$_3$H
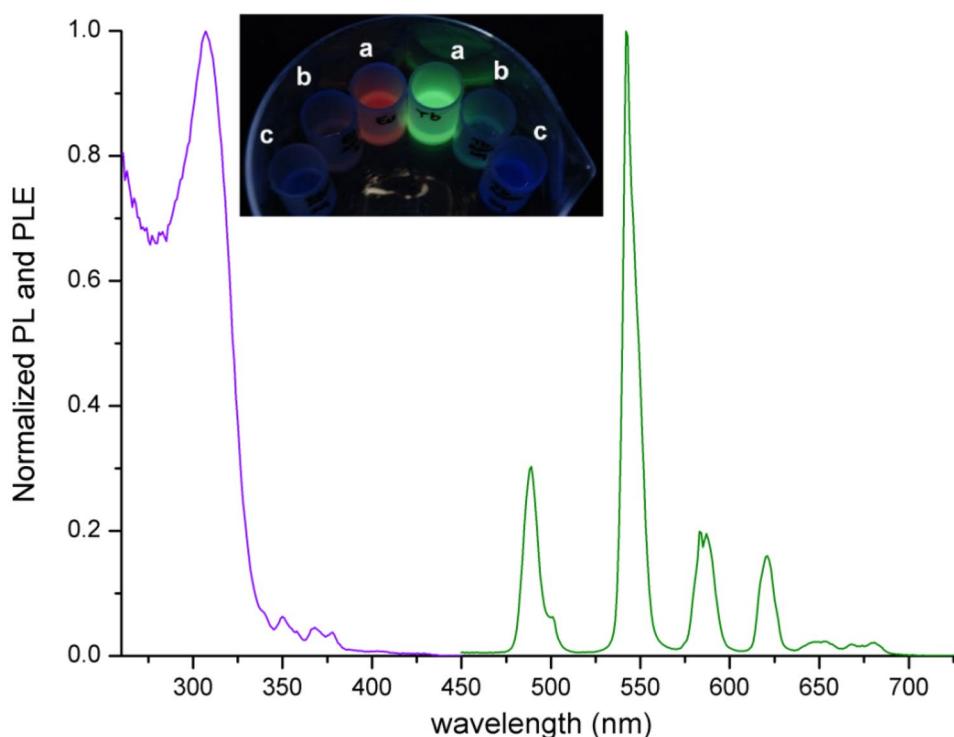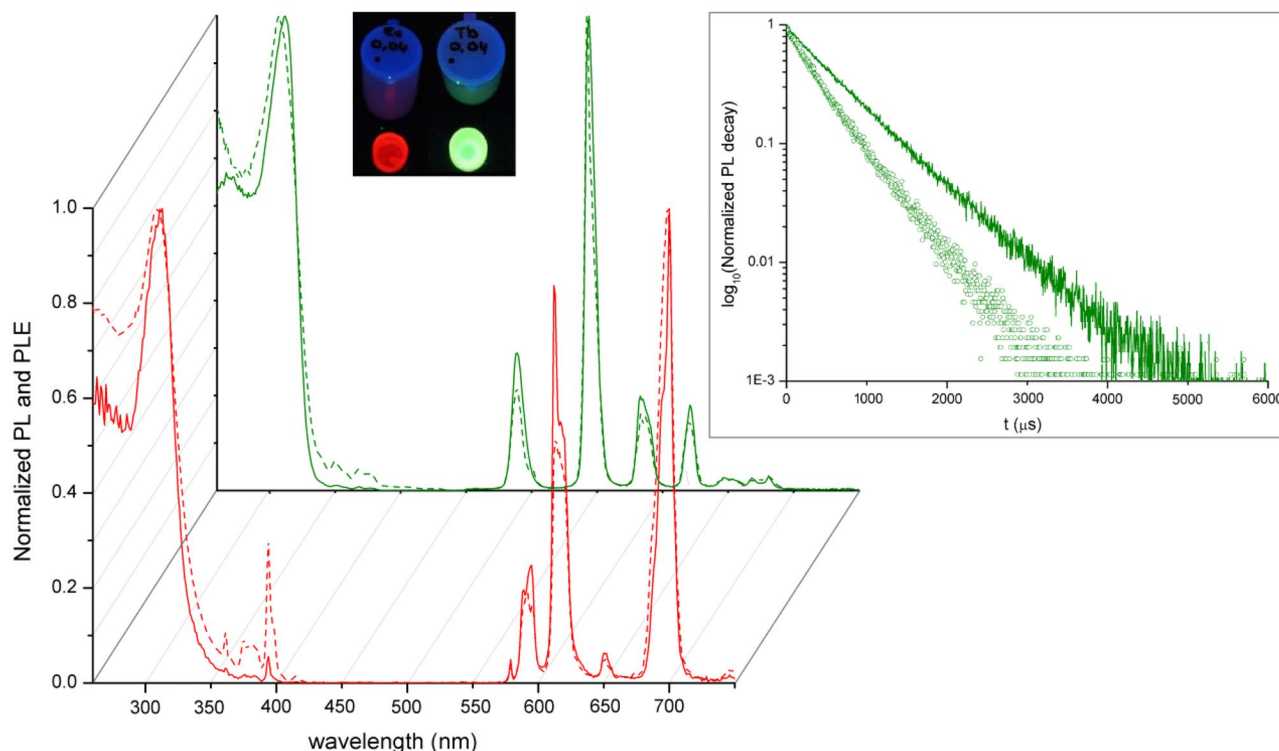
Fig. 5 PL and PLE spectra of solid [Ln(tbtz)$_3$] and [Ln(tbtz)$_3$]@ PMMA. Ln = Eu, red; Ln = Tb, green. Solid line, doped polymer; dashed line, pure complex. Inset: [Ln(tbtz)$_3$]@PMMA samples (0.040 $g_{complex}$/$g_{polymer}$) under UV irradiation. Inset: semi-log plot of the luminescence decay curves of solid [Tb(tbtz)$_3$]@PMMA (solid line) and [Tb(tbtz)$_3$] (dots), $\lambda_{excitation}$ = 320 nm, $\lambda_{emission}$ = 542 nm

maintained for [Tb(tbtz)$_3$]@PMMA. The PL spectrum of the terbium-doped material is quite similar to that of the pure complex, but the meaningful variation of the luminescence decay curve (Fig. 5) highlights also in this case the interaction of the PMMA chains with the lanthanide complex. The τ value of [Tb(tbtz)$_3$]@PMMA is 0.630 ms, longer than that of pure [Tb(tbtz)$_3$], with a consequent increase of Q_{Tb}^{Tb}, the estimated value being around 13%. The lifetime values of [Eu(tbtz)$_3$] and [Eu(tbtz)$_3$]@PMMA are instead similar, but the different PL spectra suggest that this outcome is merely a coincidence. The photoluminescence data of [Ln(tbtz)$_3$]@ PMMA materials are summarized in Table 1.

Conclusion

In this paper we described the synthesis and photo-physical characterization of luminescent europium and terbium complexes with a scorpionate ligand based on benzotriazole. The new compounds are rare examples of homoleptic tris(benzotriazol-1-yl)borate metal complexes [62]. [Eu(tbtz)$_3$] maintained the peculiar emission features already observed for the analogous tris(pyrazol-1-yl)borate derivative, in particular the unusually high intensity of the $^5D_0 \rightarrow {}^7F_4$ transition around 700 nm, in

agreement with comparable first coordination spheres. The change of the azole in the scorpionate skeleton however caused a variation in the excitation range, in the luminescence lifetimes and in the quantum yields. Moreover, the tris(benzotriazol-1-yl)borate derivatives revealed to be more influenced by the surrounding environment with respect to tris(pyrazol-1-yl)borate homoleptic complexes, making these species of potential interest in the field of luminescent sensors. Despite the fact that bright luminescent materials were obtained by embedding the complexes in poly(methyl methacrylate), the photoluminescence data clearly indicated that the coordination sphere was altered by the polymer chains.

Authors' Contributions Marco Bortoluzzi, conceptualization, validation, formal analysis, investigation, writing, funding acquisition; Valentina Ferraro, investigation, writing, formal analysis; Federica Sartor, investigation, validation.

No custom software was used. The software used is described in the Experimental Section.

Data Availability Statement The datasets generated during the current study are available from the corresponding author on reasonable request.

Declarations

Conflict of Interest There is no conflict of interest or competing interest to declare.

Open Access This article is licensed under a Creative Commons Attribution 4.0 International License, which permits use, sharing, adaptation, distribution and reproduction in any medium or format, as long as you give appropriate credit to the original author(s) and the source, provide a link to the Creative Commons licence, and indicate if changes were made. The images or other third party material in this article are included in the article's Creative Commons licence, unless indicated otherwise in a credit line to the material. If material is not included in the article's Creative Commons licence and your intended use is not permitted by statutory regulation or exceeds the permitted use, you will need to obtain permission directly from the copyright holder. To view a copy of this licence, visit http://creativecommons.org/licenses/by/4.0/.

References

1. Bünzli JCG, Piguet C (2005) Taking advantage of luminescent lanthanide ions. Chem Soc Rev 34:1048–1077. https://doi.org/10.1039/B406082M
2. Binnemans K (2009) Lanthanide-based luminescent hybrid materials. Chem Rev 109:4283–4374. https://doi.org/10.1021/cr8003983
3. Carlos LD, Ferreira RAS, de Zea BV, Julián-López B, Escribano P (2011) Progress on lanthanide-based organic-inorganic hybrid phosphors. Chem Soc Rev 40:536–549. https://doi.org/10.1039/C0CS00069H
4. Bünzli JCG, Eliseeva SV (2013) Intriguing aspects of lanthanide luminescence. Chem Sci 4:1939–1949. https://doi.org/10.1039/C3SC22126A
5. Bünzli JCG (2015) On the design of highly luminescent lanthanide complexes. Coord Chem Rev 293–294:19–47. https://doi.org/10.1016/j.ccr.2014.10.013
6. Kuriki K, Koike Y (2002) Plastic optical fiber lasers and amplifiers containing lanthanide complexes. Chem Rev 102:2347–2356. https://doi.org/10.1021/cr010309g
7. Rocha J, Carlos LD, Almeida Paz FA, Ananias D (2011) Luminescent multifunctional lanthanides-based metal-organic frameworks. Chem Soc Rev 40:926–940. https://doi.org/10.1039/C0CS00130A
8. Kido J, Okamoto Y (2002) Organo lanthanide metal complexes for electroluminescent materials. Chem Rev 102:2357–2368. https://doi.org/10.1021/cr010448y
9. Xu H, Sun Q, An Z, Wei Y, Liu X (2015) Electroluminescence from europium(III) complexes. Coord Chem Rev 293–294:228–249. https://doi.org/10.1016/j.ccr.2015.02.018
10. Zhang X, Wang T, Qin X, Zhang Z, Sun Y, Liang H, Li H (2017) Large-area flexible, transparent, and highly luminescent films containing lanthanide(III) complex-doped ionic liquids for efficiency enhancement of silicon-based heterojunction solar cell. Prog Photovolt Res Appl 25:1015–1021. https://doi.org/10.1002/pip.2915
11. Allendorf MD, Bauer CA, Bhakta RK, Houk RJT (2009) Luminescent metal-organic frameworks. Chem Soc Rev 38:1330–1352. https://doi.org/10.1039/B802352M
12. Bünzli JCG (2010) Lanthanide luminescence for biomedical analyses and imaging. Chem Rev 110:2729–2755. https://doi.org/10.1021/cr900362e
13. Eliseeva SV, Bünzli JCG (2010) Lanthanide luminescence for functional materials and bio-sciences. Chem Soc Rev 39:189–227. https://doi.org/10.1039/B905604C
14. Guo P-H, Liu J-L, Jia J-H, Wang J, Guo F-S, Chen Y-C, Lin W-Q, Leng J-D, Bao D-H, Zhang X-D, Luo J-H, Tong M-L (2013) Multifunctional Dy$^{III}_4$ cluster exhibiting white-emitting, ferroelectric and single-molecule magnet behavior. Chem Eur J 19:8769–8773. https://doi.org/10.1002/chem.201300299
15. Guo P-H, Meng Y, Chen Y-C, Li Q-W, Wang B-Y, Leng J-D, Bao D-H, Jia J-H, Tong M-L (2014) A zigzag Dy$^{III}_4$ cluster exhibiting single-molecule magnet, ferroelectric and white-light emitting properties. J Mater Chem C 2:8858–8864. https://doi.org/10.1039/C4TC01275E
16. Andres J, Hersch RD, Moser J-E, Chauvin A-S (2014) A new anti-counterfeiting feature relying on invisible luminescent full color images printed with lanthanide-based inks. Adv Funct Mater 24:5029–5036. https://doi.org/10.1002/adfm.201400298
17. Li H, Li P (2018) Luminescent materials of lanthanoid complexes hosted in zeolites. Chem Commun 54:13884–13893. https://doi.org/10.1039/C8CC07440B
18. Zheng K, Liu Z, Jiang Y, Guo P, Li H, Zeng C, Weng Ng S, Zhong S (2018) Ultrahigh luminescence quantum yield coordination polymer as a multifunctional sensor. Dalton Trans 47:17432–17440. https://doi.org/10.1039/C8DT03832E
19. Jia J-H, Li Q-W, Chen Y-C, Liu J-L, Tong M-L (2019) Luminescent single-molecule magnets based on lanthanides: design strategies, recent advances and magneto-luminescent studies. Coord Chem Rev 378:365–381. https://doi.org/10.1016/j.ccr.2017.11.012
20. Chen X, Xu Y, Li H (2020) Lanthanide organic/inorganic hybrid systems: Efficient sensors for fluorescence detection. Dyes Pigments 178:108386. https://doi.org/10.1016/j.dyepig.2020.108386
21. Reger DL, Lindeman JA, Lebioda L (1988) Synthesis, X-ray structure, and multinuclear NMR study of the dynamic behavior of tris[dihydrobis(1-pyrazolyl)borato]yttrium(III): a molecule with three three-center, two-electron bonds. Inorg Chem 27:1890–1896. https://doi.org/10.1021/ic00284a016
22. Reger DL, Lindeman JA, Lebioda L (1988) Tris(pyrazolyl) borate complexes of yttrium. X-ray crystal structures of [HB(pz)$_3$]$_2$YCl(Hpz) and {[HB(pz)$_3$]Y(μ-O2CCH3)2}2 (pz = pyrazolyl ring). Inorg Chem 27:3923–3929. https://doi.org/10.1021/ic00295a010
23. Liu S, Maunder GH, Sella A, Stevenson M, Tocher DA (1996) Synthesis and molecular structures of hydrotris(dimethylpyrazolyl) borate complexes of the lanthanides. Inorg Chem 35:76–81. https://doi.org/10.1021/ic941469w
24. Apostolidis C, Carvalho A, Domingos A, Kanellakopulos B, Maier R, Marques N, Pires de Matos A, Rebizant J (1999) Chloro-lanthanide, and plutonium complexes containing the hydrotris(3,5-dimethylpyrazol-ylborate ligand: the crystal and molecular structures of [PrCl(μ -Cl)Tp^{Me2}(3,5-Me$_2$pzH]$_2$ and YbCl$_2$Tp^{Me2}(THF). Polyhedron 18:263–272. https://doi.org/10.1016/S0277-5387(98)00294-0
25. Moss MAJ, Jones CJ, Edwards AJ (1989) Heteroleptic poly(pyrazolyl)borate derivatives of the lanthanide ions. The synthesis of acetylacetonate complexes and the molecular structures of [Ln{HB(C$_3$N$_2$H$_3$)$_3$}$_2$(MeC(O)CHC(O)Me}] (Ln = Ce or Yb). Dalton Trans 1393–1400. https://doi.org/10.1039/DT9890001393
26. Onishi M, Yamaguchi H, Shimotsuma H, Hiraki K, Nagaoka J, Kawano H (1999) Syntheses of new {tetrakis(1-pyrazolyl) borato}samarium(III) complexes and their temperature-dependent

exchange motions of all pyrazolyl groups. Chem Lett 28:573–574. https://doi.org/10.1246/cl.1999.573

27. Marques N, Sella A, Takats J (2002) Chemistry of the lanthanides using pyrazolylborate ligands. Chem Rev 102:2137–2160. https://doi.org/10.1021/cr010327y

28. Cheng J, Saliu K, Kiel GY, Ferguson MJ, McDonald R, Takats J (2008) Scorpionate-supported dialkyl and hydhydride lanthanide complexes: ligand- and solvent-dependent cluster hydride formation. Angew Chem Int Ed 47:4910–4913. https://doi.org/10.1002/anie.200705977

29. Cheng J, Saliu K, Ferguson MJ, McDonalds R, Takats J (2010) Variable nuclearity scorpionate-supported lanthanide polyhydrides: [(Tp$^{R, R'}$)Ln$_H$2]n (n = 3, 4 and 6). J Organomet Chem 695:2696–2702. https://doi.org/10.1016/j.jorganchem.2010.08.020

30. Lannes A, Luneau D (2015) New family of lanthanide-based complexes with different scorpionate-type ligands: a rare case where dysprosium and ytterbium analogues display singlet-ion magnet behavior. Inorg Chem 54:6736–6743. https://doi.org/10.1021/acs.inorgchem.5b00432

31. Kühling M, McDonald R, Liebing P, Hilfert L, Ferguson MJ, Takats J, Edelmann FT (2016) Stabilization of molecular lanthanide polysulfides by bulky scorpionate ligands. Dalton Trans 45:10118–10121. https://doi.org/10.1039/C6DT01439A

32. Bortoluzzi M, Reolon A, Scrivanti A, Enrichi F (2018) The conjugate base of malonaldehyde as antenna-ligand towards trivalent europium and terbium ions. Chem Pap 72:809–819. https://doi.org/10.1007/s11696-017-0182-z

33. Stainer MVR, Takats J (1982) X-ray crystal and molecular structure of tris[hydridotris(pyrazol-1-yl)borato]ytterbium(III), Yb(HBPz$_3$)$_3$. Inorg Chem 21:4050–4053. https://doi.org/10.1021/ic00141a034

34. Apostolidis C, Rebizant J, Kanellakopulos B, Von Ammon R, Dornberg E, Müller J, Powietska B, Nuber B (1997) Homoscorpionates (hydridotris(1-pyrazolyl)borato complexes) of the trivalent 4f ions. The crystal and molecular structure of [(HB(N$_2$C$_3$H$_3$)$_3$]$_3$Ln^{III}, (Ln = Pr, Nd). Polyhedron 16:1057–1068. https://doi.org/10.1016/S0277-5387(96)00391-9

35. Apostolidis C, Rebizant J, Walter O, Kanellakopulos B, Reddmann H, Amberger H-D (2002) Zur Elektronenstruktur hochsymmetrischer Verbindungen der f-Elemente. 35 [1] Kristall- und Molekülstrukturen von Tris(hydrotris(1-pyrazolyl)borato)-lanthanid(III) (LnTp$_3$; Ln = La, Eu) sowie Elektronenstruktur von EuTp$_3$. Z Anorg Allg Chem 628:2013–2025. https://doi.org/10.1002/1521-3749(200209)628:9/10%3c2013::AID-ZAAC2013%3e3.0.CO;2-K

36. Amberger HD, Reddmann H, Apostolidis C, Kanellakopulos B (2003) Zur Elektronenstruktur hochsymmetrischer Verbindungen der f-Elemente. 36 [1] Parametrische Analyse der optischen Spektren eines orientierten Tris(hydrotris(1-pyrazolyl)borato)praseodym(III)-Einkristalls. Z Anorg Allg Chem 629:147–160. https://doi.org/10.1002/zaac.200390008

37. Reddmann H, Apostolidis C, Walter O, Rebizant J, Amberger H-D (2005) Zur Elektronenstruktur hochsymmetrischer Verbindungen der f-Elemente. 38 [1] Kristall-, Molekül- und Elektronenstruktur von Tris(hydrotris(1-pyrazolyl)borato)-samarium(III). Z Anorg Allg Chem 631:1487–1496. https://doi.org/10.1002/zaac.200500004

38. Reddmann H, Apostolidis C, Walter O, Amberger H-D (2006) Zur Elektronenstruktur hochsymmetrischer Verbindungen der f-Elemente. 40. Parametrische Analyse des Kristallfeld-Aufspaltungsmusters von Tris(hydrotris(1-pyrazolyl)borato) neodym(III). Z Anorg Allg Chem 632:1405–1408. https://doi.org/10.1002/zaac.200600056

39. Bortoluzzi M, Paolucci G, Polizzi S, Bellotto L, Enrichi F, Ciorba S, Richards BS (2011) Photoluminescence studies on europium-based scorpionate-complex. Inorg Chem Commun 14:1762–1766. https://doi.org/10.1016/j.inoche.2011.08.004

40. Bortoluzzi M, Paolucci G, Gatto M, Roppa S, Enrichi F, Ciorba S, Richards BS (2012) Preparation of photoluminescent PMMA doped with tris(pyrazol-1-yl)borate lanthanide complexes. J Lumin 132:2378–2384. https://doi.org/10.1016/j.jlumin.2012.04.005

41. Gheno G, Bortoluzzi M, Ganzerla R, Enrichi F (2014) Inorganic pigments doped with tris(pyrazol-1-yl)borate lanthanide complexes: A photoluminescence study. J Lumin 145:963–969. https://doi.org/10.1016/j.jlumin.2013.09.027

42. Davies GM, Aarons RJ, Motson GR, Jeffery JC, Adams H, Faulkner S, Ward MD (2004) Structural and near-IR photophysical studies on ternary lanthanide complexes containing poly(pyrazolyl)borate and 1, 3-diketonate ligands. Dalton Trans 1136–1144. https://doi.org/10.1039/B400992D

43. Lu D, Tang H (2015) Theoretical survey of the ligand tunability of poly(azolyl)borates. Phys Chem Chem Phys 17:17027–17033. https://doi.org/10.1039/C5CP02094H

44. Armarego WLF, Perrin DD (1996) Purification of laboratory chemicals, 4th edn. Butterworth-Heinemann, Oxford

45. Shiu KB, Shen FM, Wang SL, Wei SC (1989) Organotransition-metal complexes of multidentate ligands: IX. Synthesis and structure of hydridotris(benzotriazol-l-yl) borate derivatives of the group VI metal carbonyls. J Organomet Chem 372:251–261. https://doi.org/10.1016/0022-328X(89)87099-8

46. Lalor FJ, Miller SM, Garvey N (1990) Poly(benzotriazolyl) borates—I. ligand synthesis and characterization. Polyhedron 9:63–68. https://doi.org/10.1016/S0277-5387(00)84248-5

47. Effendy LGG, Marchetti F, Pellei M, Pettinari C, Pettinari R, Santini C, Skelton BW, White AH (2004) Syntheses and spectroscopic and structural characterization of silver(I) complexes containing tris(isobutyl)phosphine and poly(azol-1-yl)borates. Inorg Chim Acta 357:4247–4256. https://doi.org/10.1016/j.ica.2004.06.020

48. Bain GA, Berry JF (2008) Diamagnetic corrections and Pascal's constants. J Chem Ed 85:532–536. https://doi.org/10.1021/ed085p532

49. Lin CY, George MW, Gill PMW (2004) EDF2: A Density Functional for Predicting Molecular Vibrational Frequencies. Aust J Chem 57:365–370. https://doi.org/10.1071/CH03263

50. Hay PJ, Wadt WR (1985) Ab initio effective core potentials for molecular calculations. Potentials for the transition-metal atoms Sc to Hg. J Chem Phys 82:270–283. https://doi.org/10.1063/1.448799

51. Henre WJ, Ditchfield R, Pople JA (1972) Self-Consistent Molecular Orbital Methods. XII. Further Extensions of Gaussian-Type Basis Sets for Use in Molecular Orbital Studies of Organic Molecules. J Chem Phys 56:2257–2261. https://doi.org/10.1063/1.1677527

52. Dolg M, Stoll H, Savin A, Preuss H (1989) Energy-adjusted pseudopotentials for the rare earth elements. Theor Chim Acta 75:173–194. https://doi.org/10.1007/BF00528565

53. Dolg M, Stoll H, Preuss H (1993) A combination of quasirelativistic pseudopotential and ligand field calculations for lanthanoid compounds. Theor Chim Acta 85:441–450. https://doi.org/10.1007/BF01112983

54. Cramer CJ (2004) Essentials of Computational Chemistry, 2nd edn. Wiley, Chichester

55. Shao Y, Gan Z, Epifanovsky E, Gilbert ATB, Wormit M, Kussmann J, Lange AW, Behn A, Deng J, Feng X, Ghosh D, Goldey M, Horn PR, Jacobson LD, Kaliman I, Khaliullin RZ, Kuś T, Landau A, Liu J, Proynov EI, Rhee YM, Richard RM, Rohrdanz MA, Steele RP, Sundstrom EJ, Woodcock HL III, Zimmerman PM, Zuev D, Albrecht B, Alguire E, Austin B, Beran GJO, Bernard YA, Berquist E, Brandhorst K, Bravaya KB, Brown ST, Casanova D, Chang CM, Chen Y, Chien SH, Closser KD, Crittenden DL, Diedenhofen M,

DiStasio RA Jr, Do H, Dutoi AD, Edgar RG, Fatehi S, Fusti-Molnar L, Ghysels A, Golubeva-Zadorozhnaya A, Gomes J, Hanson-Heine MWD, Harbach PHP, Hauser AW, Hohenstein EG, Holden ZC, Jagau TC, Ji H, Kaduk B, Khistyaev K, Kim J, Kim J, King RA, Klunzinger P, Kosenkov D, Kowalczyk T, Krauter CM, Lao KU, Laurent AD, Lawler KV, Levchenko SV, Lin CY, Liu F, Livshits E, Lochan RC, Luenser A, Manohar P, Manzer SF, Mao SP, Mardirossian N, Marenich AV, Maurer SA, Mayhall NJ, Neuscamman E, Melania Oana C, Olivares-Amaya R, O'Neill DP, Parkhill JA, Perrine TM, Peverati R, Prociuk A, Rehn DR, Rosta E, Russ NJ, Sharada SM, Sharma S, Small DW, Sodt A, Stein T, Stuck D, Su YC, Thom AJW, Tsuchimochi T, Vanovschi V, Vogt L, Vydrov O, Wang T, Watson MA, Wenzel J, White A, Williams CF, Yang J, Yeganeh S, Yost SR, You ZQ, Zhang IY, Zhang X, Zhao Y, Brooks BR, Chan GKL, Chipman DM, Cramer CJ, Goddard WA III, Gordon MS, Hehre WJ, Klamt A, Schaefer HF III, Schmidt MW, David Sherrill C, Truhlar DG, Warshel A, Xu X, Aspuru-Guzik A, Baer R, Bell AT, Besley NA, Chai JD, Dreuw A, Dunietz BD, Furlani TR, Gwaltney SR, Hsu CP, Jung Y, Kong J, Lambrecht DS, Liang W, Ochsenfeld C, Rassolov VA, Slipchenko LV, Subotnik JE, Van Voorhis T, Herbert JM, Krylov AI, Gill PMW, Head-Gordon M (2015) Advances in molecular quantum chemistry contained in the Q-Chem 4 program package. Mol Phys 113:184–215. https://doi.org/10.1080/00268976.2014.952696

56. Cotton S (2006) Lanthanide and Actinide Chemistry. Wiley, Chichester
57. Binnemans K (2015) Interpretation of europium(III) spectra. Coord Chem Rev 295:1–45. https://doi.org/10.1016/j.ccr.2015.02.015
58. Schubert EF (2006) Light-Emitting Diodes, 2nd edn. Cambridge University Press, Cambridge, pp 292–303
59. Bünzli JCG, Chauvin A-S, Kim HK, Deiters E, Eliseeva SV (2010) Lanthanide luminescence efficiency in eight- and nine-coordinate complexes: role of the radiative lifetime. Coord Chem Rev 254:2623–2633. https://doi.org/10.1016/j.ccr.2010.04.002
60. Vázquez-Ibar JL, Weinglass AB, Kaback HR (2002) Engineering a terbium-binding site into an integral membrane protein for luminescence energy transfer. Proc Natl Acad Sci 6:3487–3492. https://doi.org/10.1073/pnas.052703599
61. Chia YY, Tay MG (2014) An insight into fluorescent transition metal complexes. Dalton Trans 43:13159–13168. https://doi.org/10.1039/C4DT01098A
62. Güell M, Solà M, Swart M (2010) Spin-state splitting of iron(II) complexes with trispyrazolyl ligands. Polyhedon 29:84–93. https://doi.org/10.1016/j.poly.2009.06.006